

Synthesis and Characterization of CuAlS₂ Nanoparticles by Facile Heat Arrested Method

Y. Vahidshad*, R. Ghasemzadeh, A. Irajizad, M. Mirkazemi, A. Masoud

School of Metallurgy and Material Engineering, Iran University of Science and Technology, Tehran 16844, Iran

Article history:

Received 27/8/2012

Accepted 21/11/2012

Published online 1/12/2012

Keywords:

Heat arrested method

Poly alcohol

Chalcopyrite

Sulfide copper

Semiconductor

*Corresponding author:

E-mail address:

yvahidshad@iust.ac.ir

Phone: 98 912 4515282

Fax: +98 21 66282146

Abstract

CuAlS₂ Chalcopyrite nanocrystalline are synthesized with facile method. The heat arrested solvothermal method for synthesise nanocrystalline were investigated. The time duration of synthesis, temperature of solution and metal salts to solvent molar ratio can be parameters that we are studied. The nanoparticles were synthesized with CuCl, AlCl₃ and thiourea (SC(NH₂)₂) as precursors, Diehylene glycol ((CH₂CH₂OH)₂O) and Polyethylene glycol 600 (HO(C₂H₄O)_nH) as solvent and capping agent respectively, and Ammonia (NH₄OH) as reducing agent. The parameters of synthesis were studied by X-Ray diffraction (XRD) for analysis of structure and by ultraviolet-visible (UV-VIS) spectrophotometer for analysis of light structure. The possible formation mechanism metal complexes, sulfur ions and chalcopyrite compound are also discussed.

2012 JNS All rights reserved

1. Introduction

Semiconducting chalcopyrite compounds have been received special interest because of the optical, electrical and structural properties can simply be wide-ranging at large extent by varying of chemical and stoichiometry. In the I-III-VI₂ compounds (chalcopyrite), the linear and nonlinear optical properties, the kind of electrical conductivity and the band gap can be changed with change of intrinsic composition ratio and can be covering the wide applications in the semiconducting industry. Among in the

chalcopyrite semiconductors, CuAlS₂ compounds have a wide band gap around the 3.5eV that useful for ultraviolet absorption [1-5].

There are to general methods to achieve the chalcopyrite structure. The first method is the use of H₂S gas for passing from the through of intermetallic compounds. The second method is use of wet chemical synthesis for chalcopyrite compounds. In these chemical processes there are not time-consuming, expensive, and complexity of process beside of the large material losses [6-12]. At among of wet chemical synthesis, polyol

method is the best because the control of stoichiometry is simpler and the powders synthesized have well crystalline without any post heat treatment [13]. At polyol method we used from high boiling solvent (Oley amine, Diethylene glycol, Diethanolamine and etc.) and the pressure is ambient pressure. Their method involved the reduction of precursors in the presence of capping agent (Oleic acid, Polyethylene glycol, etc) [14]. The chalcopryrite material such as $\text{CuIn}_x\text{Ga}_{1-x}\text{S}_2$, CuInS_2 , CuAlS_2 and CuFeS_2 is more environmental friendly than selenide chalcopryrite. Nowadays, a low cost technique for the synthesis of the non-toxic chalcopryrite nanoparticles is most important

for photovoltaic or light emitting diode industries [15, 16]. In this research, we investigated the solvothermal reaction without autoclave (polyol) for CuAlS_2 chalcopryrite. We are researching about the effect of different reaction conditions on the chalcopryrite formability and structural and optical properties of this compound.

2. Experimental procedure

The precursors used in this process are used copper dichloride, CuCl_2 ; aluminum trichloride, AlCl_3 ; thiourea; Diethylene glycol (DEG), Polyethylene glycol 600 (PEG) and Ammonia.

Table 1. Experimental detail for polyol method.

Sample No.	Salt mmol:Solvent mmol	Amount of reducer	Synthesis Duration	Reducer Temp. (°C)	Salts Temp. (°C)	pH
CAS-WOA-1	(10+10) mmol:316 mmol	5 cc (Ammonia)	8 hr	120-140	120-140	10
CAS-WOA-2	(10+10) mmol:316 mmol	5 cc (Ammonia)	16 hr	120-140	120-140	10
CAS-WOA-3	(10+10) mmol:316 mmol	5 cc (Ammonia)	24 hr	120-140	120-140	10
CAS-WOA-4	(10+10) mmol:316 mmol	5 cc (Ammonia)	16 hr	20-30	120-140	13.5
CAS-WOA-5	(10+10) mmol:316 mmol	10 cc (Ammonia)	16 hr	20-30	120-140	12
CAS-WOA-6	(10+10) mmol:316 mmol	2 cc (Ammonia)	16 hr	20-30	120-140	11
CAS-WOA-7	(10+10) mmol:316 mmol	10 cc (Ammonia)	16 hr	20-30	120-140	13.5
CAS-WOA-8	(10+10) mmol:316 mmol	15cc (Ammonia)	16 hr	20-30	120-140	13.5
CAS-WOA-9	(10+10) mmol:316 mmol	20cc (Ammonia)	16 hr	20-30	120-140	13.5
CAS-WOA-10	(10+10) mmol:316 mmol	20 cc (EDA)	16 hr	20-30	120-140	14
CAS-WOA-11	(10+10) mmol:316 mmol	20 cc (DEA)	16 hr	20-30	120-140	12
CAS-WOA-12	(10+10) mmol:316 mmol	10 cc (Ammonia)	16 hr	20-30	20-30	12.5
CAS-WOA-13	(10+10) mmol:316 mmol	20 cc (Ammonia)	16 hr	20-30	20-30	12.5
CAS-WOA-14	(10+10) mmol:316 mmol	30 cc (Ammonia)	16 hr	20-30	20-30	13
CAS-WOA-15	(10+10) mmol:316 mmol	10 cc (Ammonia)	16 hr	20-30	20-30	13
CAS-WOA-16	(10+10) mmol:316 mmol	20 cc (Ammonia)	16 hr	20-30	60-70	12.5
CAS-WOA-17	(10+10) mmol:316 mmol	30 cc (Ammonia)	16 hr	20-30	60-70	13
CAS-WOA-18	(3+3) mmol:316 mmol	20 cc (Ammonia)	16 hr	20-30	60-70	13
CAS-WOA-19	(3+3) mmol:316 mmol	20 cc (Ammonia)	16 hr	20-30	60-70	13
CAS-WOA-20	(1+1) mmol: 316 mmol	20cc (Ammonia)	16 hr	20-30	60-70	12.5
CAS-WOA-21	(1+1) mmol:316 mmol	40cc (Ammonia)	16 hr	20-30	60-70	13.5

In another vessel, the 40mmol thiourea and amount of reducing agent were dissolved into 10cc DEG and stirred for at least 60min to obtain a transparent solution (Solution no. 2). After that the solution no. 2 was injected into solution 1 at the defined temperatures and stirred for 15 minute. The

solution in the flask quickly turned black color and the coprecipitation reaction lasts for several minutes. After that the temperature was gained to 200-220°C for a specified time to achieve crystalline powders. When it was cooled down to room temperature, the products were centrifuged,

washed several times by distilled water and ethanol and finally dried at 60°C for 10hr at air condition. See Table 1 for details concerning solution preparation. The structural and the optical properties of the CuAlS₂ nanoparticles were characterized using X-ray diffraction spectrometer (XRD, Panalytical MPD), scanning electron microscope (SEM, Hitachi S-4800), and UV-Visible spectrophotometer (Ocean Optics In. USB-4000 optic spectrometer).

3. Results and discussion

The reaction follows an oxidation/reduction rule, in which AlCl₃ and CuCl are reduced by the strong reducer NH₄OH. The electrochemical and E° for every half-reaction is given by:

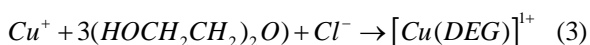
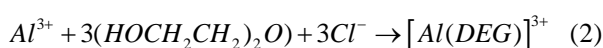
$$E^0(Cu^+ \rightarrow Cu) = +0.5180V$$

$$E^0(Al^{3+} \rightarrow Al) = -1.660V$$

$$E^0(2NH_4OH \rightarrow N_2 + H_2O + 6H^+) = -0.092V$$

$$E_{red}^0(\text{reduction process}) - E_{red}^0(\text{oxidation process}) < 0 \quad (1)$$

The high chemical potential gap of the two half reactive species (equation 1) and high temperature of solvent provides a strong reaction dynamic. then this is resulted to produce a supersaturation large enough to overcome the energy barrier of nucleation as a reductive agent is injected in. Amount of reducer is very important because the standard reduction potential for Al³⁺ is more negative than to ammonia and we need adequate amounts of ammonia for reducing of aluminum ions. The mechanism of reaction in this polyol method can be described as following. At solution of 1, the metals salt was solved as ion and then was complex with DEG (equation 2, 3):



Also, the PEG as a capping agent forms stable complexes with the precursor on the nanocrystal surface (carboxylic COOH and amine NH₂ ligands), which slows the nucleation and growth process, leading to reducing the reaction rate (fig.1):

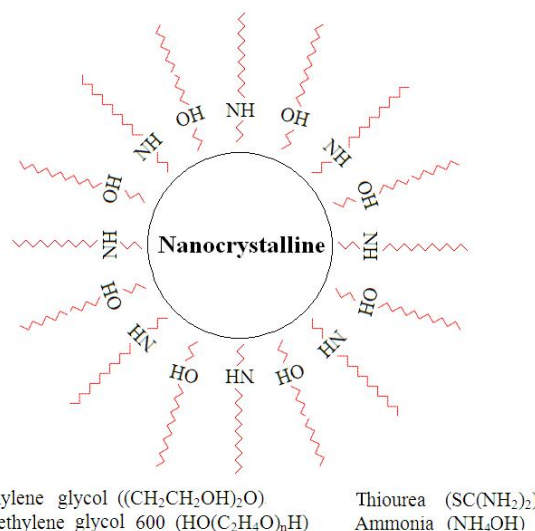
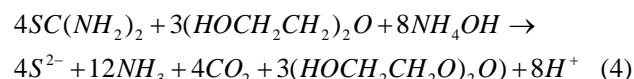
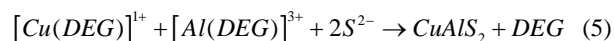


Fig.1. Schematic of capping agent forms.

At solution no. 2, the thiourea and NH₄OH have been solved as ion and reducing agent and ion of S²⁻ is formed:



When the solution no. 2 (equation 4) is injected into the solution no. 1, fast nucleation is followed by slower nanocrystal growth. This reaction mechanism can be explained based on formation of [Cu(DEG)₂]¹⁺ and [Al(DEG)₂]³⁺ complex and then decomposition and reaction with S²⁻ for formation of chalcopyrite nanocrystal:



After nanocrystals formation (equation 5), environment situation (high temperature) derives the sample to reach a crystalline phase. The effect of salt to solvent molar ration and amount of reducer was founded more important at the all of

the other parameters. In the first stage of experimental design, we study the effect of heat treatment duration and pH on the chalcopyrite formability. Figure 2a shows the chalcopyrite was formed very weakly and the Cu_xS (JCPDS 23-0960, 23-0961, 36-0380 and 33-0489) was the major phase (CAS-WOA-1 to 6). In second stage, three of samples (CAS-WOA-7, 8 and 9), we used more amount of reducer for study of chalcopyrite formability but the copper sulfide still was the major phase and the chalcopyrite was formed too weakly. Also we used from different type of reducer and we have seen no change in the chalcopyrite formability CAS-WOA-10 and 11 samples (figure 2b). In the third stage we synthesized six samples with more amount of reducer than before but still chalcopyrite phase was formed weaker than copper sulfide (figure 3a). At least, in the fourth stage, according to previous results we founded the salt to solvent molar ratio was the most influence in the synthesis and formability of aluminum chalcopyrite structure. As a result, we synthesized four samples with lower amount of precursors in the solvent.

Figure 3b shows that the chalcopyrite structure forms in these samples. The CAS-WOA-21 was the best condition synthesis for chalcopyrite formability (JCPDS 25-0014) and the three main peaks and planes of chalcopyrite structure were at 47.941 (220), 29.262 (112), 59.379 (116). The calculation results such as peak position, lattice constant, crystalline size and the tetragonal distortion were given in table 2. However, from all of the synthesized samples observed that the lateral phase copper sulfide was formed in the any condition, but it could be more or less according to the test conditions. The crystallite size could be determined by considering full width of main diffraction peak in Scherrer equation [17]:

$$d = \frac{0.9\lambda}{\beta \cos\theta} \quad (6)$$

The calculation results are given in table 2 and show that the size of the all samples is nanometer.

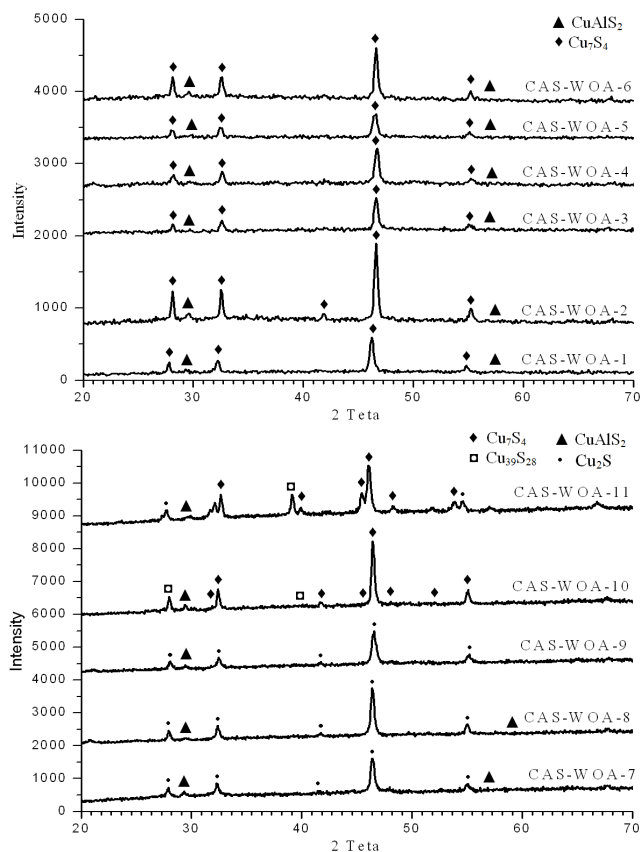


Fig 2. X-ray diffraction patterns of CuAlS_2 for (a) first stage and (b) second stage experimental design.

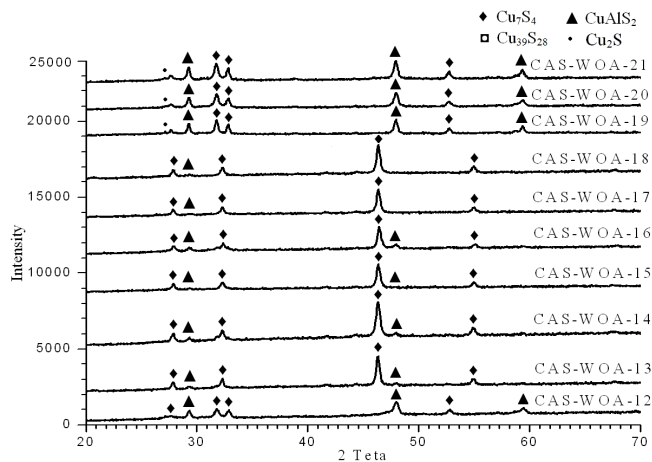


Fig 3. X-ray diffraction patterns of CuAlS_2 for third stage and fourth stage experimental design.

Table 2. Experimental detail for polyol method.

Sample No.	Position 2 θ	Height	PWHM 2 θ	d-spacing (\AA)	Related Intensity	Crystalline Size (nm)	Plane (hkl)	Structure	$\eta=c/a$ (\AA) a (\AA) c (\AA)
CAS-WOA-1	29.2881	31.65	0.5904	3.05	6.80	-	(112)	CuAlS ₂	$\eta=1.8503$
	46.2134	465.82	0.3936	1.96	100.00	45.8	(224)	Cu ₇ S ₄	a=5.429
	54.8075	78.65	0.5904	1.67	16.88	-	(422)	Cu ₇ S ₄	c=10.04
CAS-WOA-2	29.5745	83.02	0.3936	3.02	7.93	-	(112)	CuAlS ₂	$\eta=1.8019$
	46.5938	1046.25	0.3936	1.95	100.00	64.23	(224)	Cu ₇ S ₄	a=5.429
	55.2310	152.15	0.5904	1.66	14.54	-	(422)	Cu ₇ S ₄	c=9.95
CAS-WOA-3	29.6439	22.52	0.5904	3.01	5.27	-	(112)	CuAlS ₂	$\eta=1.9061$
	46.5645	427.23	0.3936	1.95	100.00	45.88	(2131)	Cu ₇ S ₄	a=5.307
	49.8121	7.20	0.3936	1.83	1.69	-	(204)	CuAlS ₂	c=10.12
CAS-WOA-4	29.6112	26.49	0.3936	3.02	5.94	-	(112)	CuAlS ₂	$\eta=1.9105$
	46.6763	446.03	0.5904	1.95	100	30.62	(2,13,1)	Cu ₂ S	a=5.308
	55.2180	75.59	0.3936	1.66	16.95	-	(286)	Cu ₂ S	c=10.14
CAS-WOA-5	29.6189	18.01	0.7872	3.02	5.92	-	(112)	CuAlS ₂	$\eta=1.9067$
	46.4458	304.12	0.4920	1.95	100	36.72	(2,13,1)	Cu ₂ S	a=5.317
	48.4352	11.66	0.5904	1.88	3.83	-	(220)	CuAlS ₂	c=10.14
CAS-WOA-6	29.5273	56.08	0.5904	3.02	7.98	-	(112)	CuAlS ₂	$\eta=1.8787$
	46.5952	702.92	0.3936	1.95	100	45.95	(2,13,1)	Cu ₂ S	a=5.346
	48.0574	38.42	0.5904	1.89	5.47	-	(220)	CuAlS ₂	c=10.04
CAS-WOA-7	29.3618	107.98	0.3936	3.04	10.53	-	(112)	CuAlS ₂	$\eta=1.9137$
	32.3701	313.87	0.4723	2.77	30.62	-	(004)	Cu ₇ S ₄	a=5.346
	46.4420	1025.21	0.4723	1.95	100.00	36.61	(224)	Cu ₇ S ₄	c=10.23
CAS-WOA-8	29.5143	48.57	0.4723	3.03	3.65	-	(112)	CuAlS ₂	$\eta=1.8425$
	32.4073	340.89	0.4723	2.76	25.60	-	(004)	Cu ₇ S ₄	a=5.402
	46.4409	1331.73	0.4723	1.95	100.00	36.70	(224)	Cu ₇ S ₄	c=9.95
CAS-WOA-9	29.4895	82.28	0.4723	3.03	8.84	-	(112)	CuAlS ₂	$\eta=1.8961$
	46.5733	930.78	0.6298	1.95	100	27.50	(224)	Cu ₇ S ₄	a=5.346
	55.1138	194.74	0.3936	1.67	20.92	-	(312)	CuAlS ₂	c=10.13
CAS-WOA-10	29.4290	271.08	0.1026	3.03	16.06	-	(112)	CuAlS ₂	$\eta=1.9649$
	32.4484	503.73	0.4723	2.76	29.85	-	(004)	Cu ₇ S ₄	a=5.280
	46.4888	1667.52	0.4723	1.95	100.00	36.71	(224)	Cu ₇ S ₄	c=10.36
CAS-WOA-11	29.7593	64.01	0.6298	3.00	4.81	-	(112)	CuAlS ₂	$\eta=1.8718$
	46.1451	1331.02	0.4723	1.97	100.00	36.66	(2,13,1)	Cu ₂ S	a=5.317
	48.3325	140.34	0.4723	1.88	10.54	-	(220)	CuAlS ₂	c=9.95
CAS-WOA-12	29.3256	442.39	0.4723	3.05	58.02	-	(112)	CuAlS ₂	$\eta=1.9317$
	31.8504	548.20	0.3936	2.81	71.89	-	(220)	Cu ₇ S ₄	a=5.346
	48.0091	762.54	0.4723	1.89	100.00	36.82	(220)	CuAlS ₂	c=10.33
CAS-WOA-13	29.3142	135.42	0.3936	3.05	7.65	-	(112)	CuAlS ₂	$\eta=1.9317$
	32.2815	503.60	0.4723	2.77	28.43	-	(004)	Cu ₇ S ₄	a=5.346
	46.3491	1771.29	0.4723	1.96	100.00	36.59	(224)	Cu ₇ S ₄	c=10.33
CAS-WOA-14	29.3276	172.51	0.4723	3.04	7.93	-	(112)	CuAlS ₂	$\eta=1.8856$
	32.3121	602.11	0.4723	2.77	27.68	-	(004)	Cu ₇ S ₄	a=5.374
	46.3651	2175.26	0.4723	1.96	100.00	36.68	(224)	Cu ₇ S ₄	c=10.13
CAS-WOA-15	29.3083	85.28	0.4723	3.05	6.08	-	(112)	CuAlS ₂	$\eta=1.9510$
	32.3180	411.51	0.4723	2.77	29.34	-	(004)	Cu ₇ S ₄	a=5.327
	46.3918	1402.36	0.4723	1.96	100.00	36.60	(224)	Cu ₇ S ₄	c=10.39
CAS-WOA-16	29.3169	173.78	0.4723	3.05	13.71	-	(112)	CuAlS ₂	$\eta=1.9030$
	32.4345	337.13	0.6298	2.76	26.60	-	(134)	Cu ₂ S	a=5.374
	46.4737	1267.33	0.4723	1.95	100.00	36.61	(224)	Cu ₇ S ₄	c=10.23
CAS-WOA-17	29.2409	72.19	0.4723	3.05	5.16	-	(112)	CuAlS ₂	$\eta=1.9636$
	32.3088	407.30	0.4723	2.77	29.12	-	(220)	Cu ₇ S ₄	a=5.316
	46.3935	1398.77	0.4723	1.96	100.00	36.60	(224)	Cu ₇ S ₄	c=10.437
CAS-WOA-18	29.3270	82.72	0.4723	3.04	4.55	-	(112)	CuAlS ₂	$\eta=1.9875$
	32.3302	468.79	0.4723	2.77	25.79	-	(220)	Cu ₇ S ₄	a=5.276
	46.3786	1817.82	0.3936	1.96	100.00	36.60	(224)	Cu ₇ S ₄	c=10.49
CAS-WOA-19	29.2891	367.61	0.6298	3.05	47.14	-	(112)	CuAlS ₂	$\eta=1.9030$
	31.7903	779.84	0.4723	2.80	100	-	(220)	Cu ₇ S ₄	a=5.374
	47.9501	779.09	0.4723	1.90	99.90	36.82	(220)	CuAlS ₂	c=10.23
CAS-WOA-20	29.2818	589.36	0.4723	3.04	69.60	-	(112)	CuAlS ₂	$\eta=1.9137$
	31.7877	789.47	0.4723	2.81	93.23	-	(220)	Cu ₇ S ₄	a=5.346
	47.9736	846.76	0.4723	1.89	100	36.82	(220)	CuAlS ₂	c=10.23
CAS-WOA-21	29.2621	696.65	0.4723	3.05	67.78	-	(112)	CuAlS ₂	$\eta=1.9030$
	32.810	952.00	0.3550	2.73	92.63	-	(044)	Cu ₂ S	a=5.374
	47.9416	1027.75	0.4723	1.90	100	36.80	(220)	CuAlS ₂	c=10.23

The optical properties of nanocrystalline are determined from absorbance measurement in the range of 200–1100nm carried out on the colloidal nanocrystalline. The absorption coefficient (α) could be obtained from Beer–Lambert law:

$$\alpha = -\frac{1}{d} \ln \left(\frac{I}{I_0} \right) \Rightarrow \alpha = 2.303 \times \frac{A}{d} \quad (7)$$

Where A is absorption of nanocrystallite obtained from spectrometer and d is a nanocrystallite diameter (equation 7). The band gap is determined from Tauc's equation:

$$(\alpha h\nu)^n = c(h\nu - E_g) \quad (8)$$

Where c is a constant, E_g was the band gap, n is the index indicating the type of the transition. It is known that the values of n for direct, indirect, forbidden direct and indirect optical transitions in equation 8 are 0.5, 2, 1.5 and 3, respectively [18-21].

Figure 4 to 7 are the plots of absorbance against wavelength in the UV and VIS region for samples CAS-WOA-1 to CAS-WOA-21. The derived data from pictures shows that the chalcopyrite phase

and most phases of Cu_xS ($x=1-2$) are existed in the synthesized samples. The edge of absorbance in the around the 324-369nm is for CuAlS_2 chalcopyrite but Cu_xS compounds show different values of the optical properties for each phase.

At this research, two absorption regions can be observed for Cu_xS in the absorption graphs; the widening of the 383-664nm and 747-1002nm is for Cu_xS compounds. This wide of absorbance is based on type of Cu_xS formability such as Cu_2S , Cu_7S_4 , $\text{Cu}_{39}\text{S}_{28}$ and $\text{Cu}_{1.765}\text{S}$. Table 3 shows the absorption edge and band gap for all of the synthesized samples. The samples were dispersed in a mixture of methanol and ethylene glycol under intense sonication of 15 min and also a mixture as a reference (the samples were dispersed with 0.3mg/ml). The band gap of samples is calculated by MATLAB software based on the data derived from UV-Vis spectrophotometer data. Also, the optical band gap of synthesized nanocrystalline can be calculated from the extrapolation of the linear portion of the $(\alpha h\nu)^2$ plots versus $h\nu$ to $\alpha = 0$.

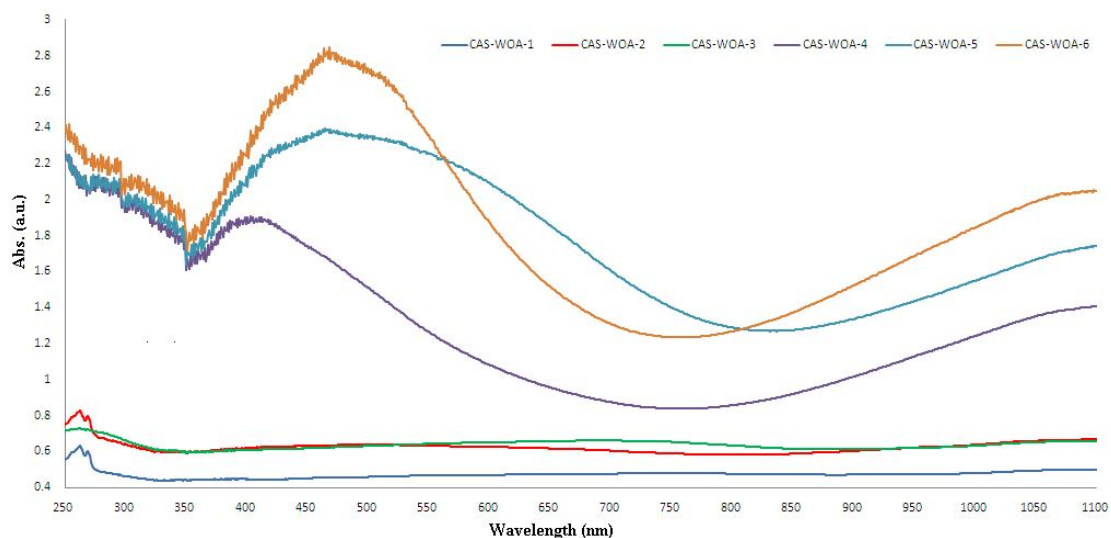


Fig. 4. UV-Vis spectra determined for first experimental design of synthesized samples.

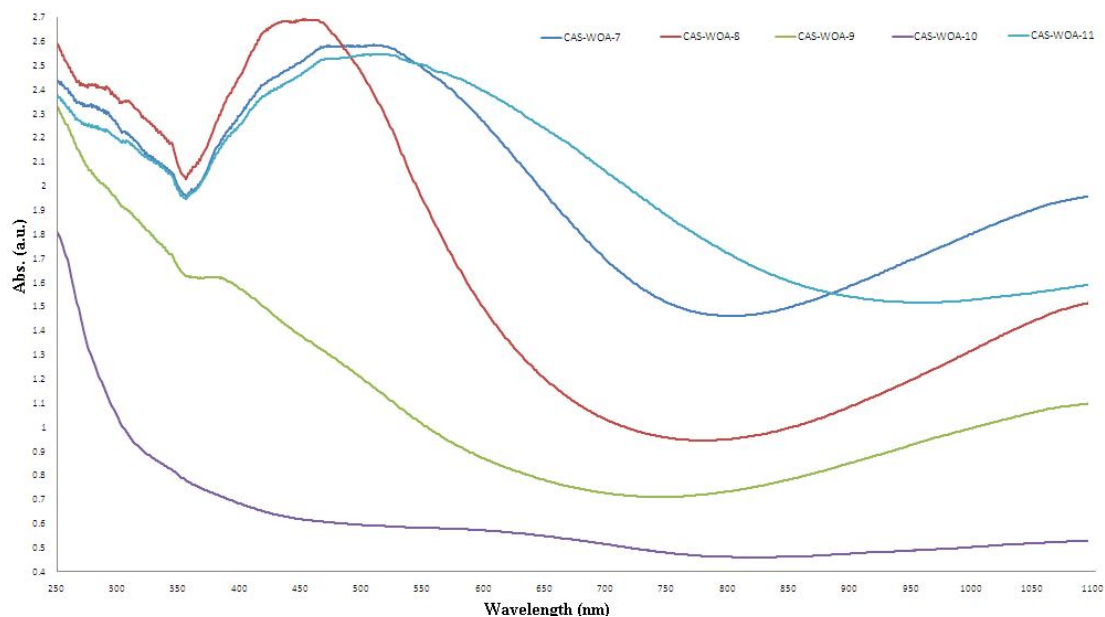


Fig. 5. UV-Vis spectra determined for second experimental design of synthesized samples.

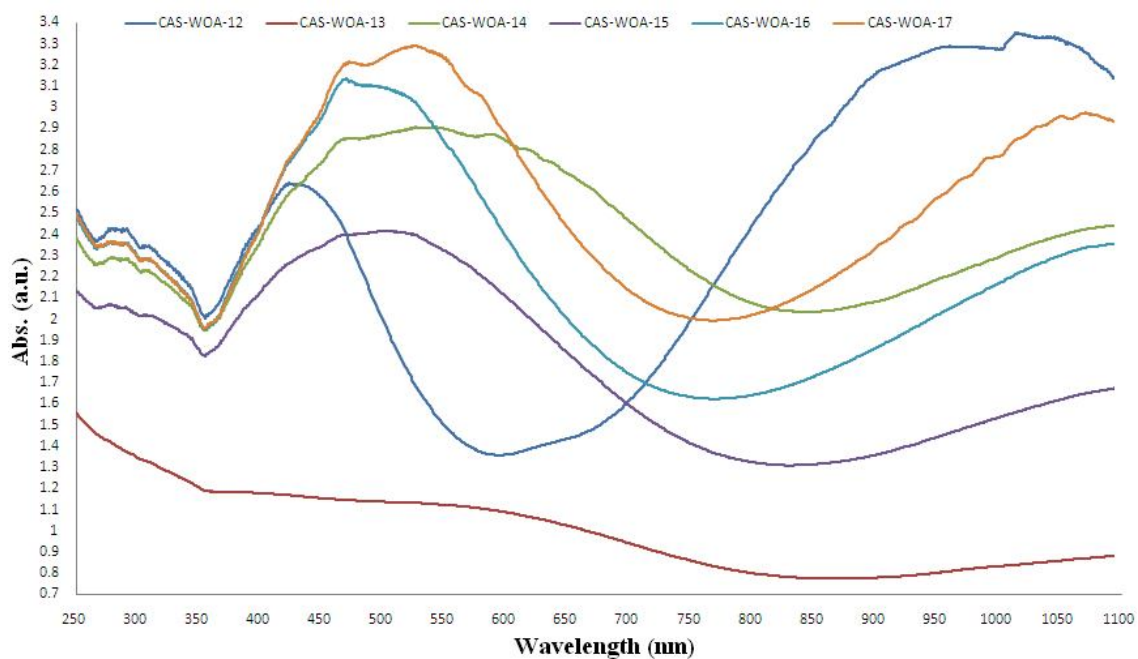


Fig.6. UV-Vis spectra determined for third experimental design of synthesized samples.

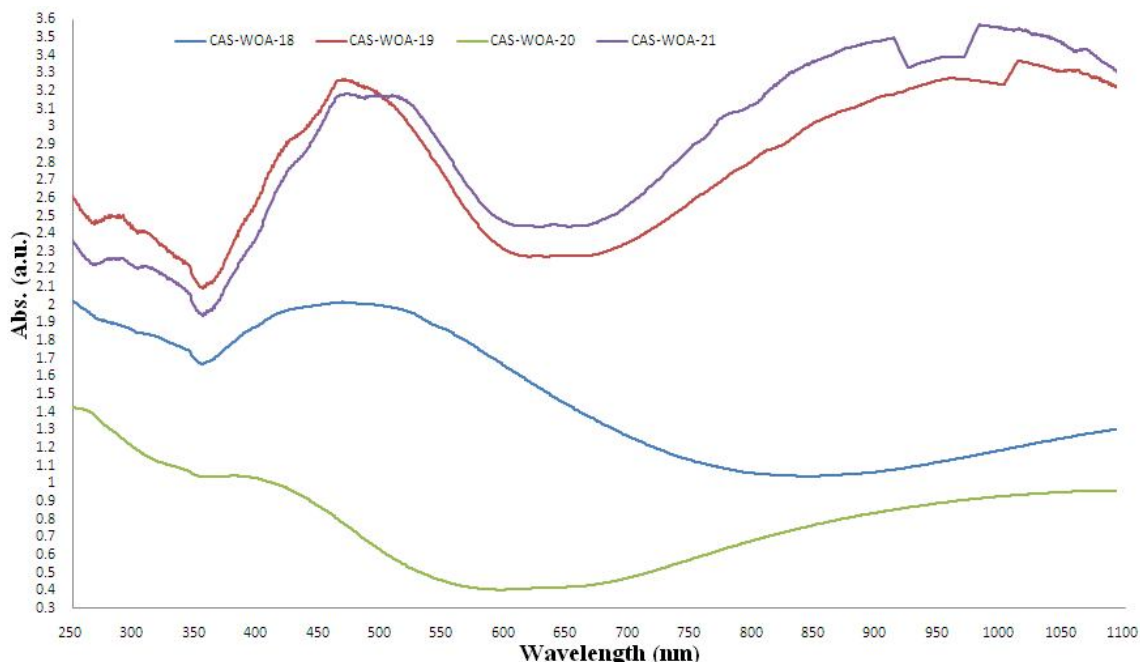


Fig.7. UV-Vis spectra determined for fourth experimental design of synthesized samples.

Table 3. UV-Vis results for synthesized samples

Sample No.	Edge of Absorption (nm)			Band gap (eV)		
	CuAlS ₂	Cu _x S compounds		CuAlS ₂	Cu _x S compounds	
CAS-WOA-1	324	410	890	4.14	2.98	1.33
CAS-WOA-2	347	440	808	4.08	3.05	1.22
CAS-WOA-3	353	446	891	3.33	3.07	1.21
CAS-WOA-4	353	446	769	3.82	2.82	2.09
CAS-WOA-5	354	433	839	3.70	2.79	1.56
CAS-WOA-6	353	446	761	3.48	2.80	1.88
CAS-WOA-7	355	514	807	3.34	2.65	1.64
CAS-WOA-8	354	458	748	3.64	2.77	1.88
CAS-WOA-9	353	383	747	3.70	2.82	1.76
CAS-WOA-10	369	-	838	4.13	2.60	1.27
CAS-WOA-11	354	505	947	3.42	2.63	1.43
CAS-WOA-12	355	590	1002	3.79	2.72	2.24
CAS-WOA-13	358	-	880	4.26	2.86	1.45
CAS-WOA-14	356	575	841	3.66	2.64	1.38
CAS-WOA-15	355	-	833	3.45	2.50	1.60
CAS-WOA-16	356	-	772	3.71	2.71	1.75
CAS-WOA-17	356	483	770	3.71	2.71	1.36
CAS-WOA-18	355	-	849	3.50	2.60	1.67
CAS-WOA-19	355	664	1002	3.68	2.75	1.87
CAS-WOA-20	358	599	-	3.51	2.66	2.30
CAS-WOA-21	355	623	925	3.65	2.56	1.84

Figure 8 shows curves of $(\alpha h\nu)^2$ vs. $h\nu$ for the CuAlS₂ nanocrystalline. Based on table 3, the

direct energy gap E_g of the nanocrystalline has been calculated and there are between 3.33 to 4.26eV. The difference in band gap calculated may be attributed to shallow level (i.e., donor and acceptor level) present in between the valence and conduction bands or effect of crystalline size.

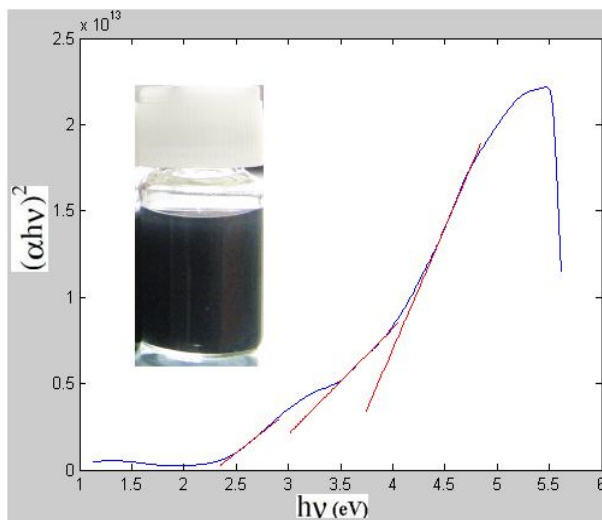


Fig.3. The plot of $(\alpha h\nu)^2-h\nu$ for CAS-WOA-20.

4. Conclusion

In this paper we reported the preparation of the CuAlS₂ chalcopyrite nanocrystalline using the polyol method. Complex mixtures of copper sulfides (Cu_xS, x=1-2) and aluminum chalcopyrite were obtained. X-ray diffraction pattern confirms that the molar ratio of salt to the solvent and the reducer solvent are very effective on the formation of the chalcopyrite phase. The lateral phase copper sulfide is formed in every situation, but in optimal conditions of synthesis of the copper sulfide chalcopyrite phase has the highest value. The optimal conditions for synthesis are as follows: molar ratio of metal salts to DEG is 2 to 316. Also, the amount of ammonia as reducer is 20cc for 2mmol of metal salts.

Acknowledgment

This work has been financially supported by Engineering Research Institute and Iran University of Science and Technology and Sharif University of Technology.

References

- [1] S. Kodigala, Cu(In_{1-x}Ga_x)Se₂ Based Thin Film Solar Cells, Academic Press, 2010.
- [2] G. Harichandran, N.P. Lalla, Materials Letters 62 (2008) 1267–1269.
- [3] M. Caglar, S. Ilican, Y. Caglar, Optics Communications 281 (2008) 1615–1624.
- [4] G.H. Yue, X. Wang, L.S. Wang, W. Wang, D.L. Peng, Physics Letters A 372 (2008) 5995–5998.
- [5] Yu-Hsiang A. Wang, N. Bao, A. Gupta, Solid State Sciences 12 (2010) 387–390.
- [6] G. Chen, L. Wang, X. sheng, H. Liu, X. Pi, D.Yang, Journal of alloys and compounds, (2010) 317-321.
- [7] G. Chen, L. Wang, X. sheng, D.Yang, Journal of sol-gel science and technology 58 (2011) 162-169.
- [8] P. Luo, P. Yu, R. Zuo, J.Jin, Y. Ding, J. Song, Y. Chen, Physica B 405 (2010) 3294-3298.
- [9] M. S. Park, S. Y. Han, E.J. Lee, C. H. Chang, S. O. Ryu, Current Applied Physics 10 (2010) 5379-5382.
- [10] H. Wei, W. Guo, Y. Sun, Z. Yang, Y. Zhang, Materials letters 64 (2010) 1424-1426.
- [11] J. Zhou, S. Li, X. Gong, Y. Yang, L. You, Y. Guo, Materials Lettes 65 (2011) 3465-3467.
- [12] A. E. Pop, V. Popescu, M. Danila, M. N. Batin, Chalcogenide Letters 8 (2011) 363 – 370.
- [13] B. L. Cushing, V. L. Kolesnichenko, and C. J. O'Connor, Chemical Reviews 104 (2004) 3893–3946.
- [14] M. S. Park, S. Y. Han, E. J. Bae, T. J. Lee, C. H. Chang, S. O. Ryu, Current Applied Physics 10 (2010) S379–S382.
- [15] C. Steinhagen, M. G. Panthani, V. Akhavan, B. Goodfellow, B. Koo, B. A. Korgel, Journal of American Chemical Society, (2009), 131, 12554–12555.
- [16] L. Z. Pei, J. F. Wang, X. X. Tao, S. B. Wang, Y. P. Dong, C. G. Fan, Q. F. Zhang, Materials Characterization 62 (2011) 354 – 359.
- [17] A.L. Fahrenbruch, R.H. Bube, Fundamentals of Solar Cells, Academic Press, New York, 1983.
- [18] R. Swanepoel, J. Phys. E: Sci. Instrum. 16 (1983) 1214-1222.
- [19] A.E. Rakhshani, J. Appl. Phys. 81 (1997) 7988-7993.
- [20] N. Jamali, M. M. B. Mohagheghee, A. Youssefi, Iranian Physics Conference, Condensed Matter: Nano-Structures (2011) 1383-1386.
- [21] S. Han, M. Kong, Y. Guo, M. Wang, Materials Letters 63 (2009) 1192–1194.